

# Hourglass dispersion in overdoped single-layered manganites

H. Ulbrich,<sup>1,\*</sup> P. Steffens,<sup>2</sup> D. Lamago,<sup>3,4</sup> Y. Sidis,<sup>4</sup> and M. Braden<sup>1,†</sup>

<sup>1</sup>*II. Physikalisches Institut, Universität zu Köln, Zùlpicher Str. 77, D-50937 Köln, Germany*

<sup>2</sup>*Institut Laue-Langevin, BP 156, 38042 Grenoble Cedex 9, France*

<sup>3</sup>*Forschungszentrum Karlsruhe, Institut für Festkörperphysik, P.O.B. 3640, D-76021 Karlsruhe, Germany*

<sup>4</sup>*Laboratoire Léon Brillouin, C.E.A./C.N.R.S., F-91191 Gif-sur-Yvette Cedex, France*

(Dated: August 6, 2018)

The incommensurate stripe-like magnetic ordering in two single-layered manganites,  $\text{Nd}_{0.33}\text{Sr}_{1.67}\text{MnO}_4$  and  $\text{Pr}_{0.33}\text{Ca}_{1.67}\text{MnO}_4$ , is found to exhibit an hourglass-like excitation spectrum very similar to that seen in various cuprates superconductors, but only for sufficiently short correlation lengths. Several characteristic features of an hourglass dispersion can be identified: enhancement of intensity at the merging of the incommensurate branches, rotation of the intensity maxima with higher energy transfer, and suppression of the outwards-dispersing branches at low energy. The correlation length of the magnetic ordering is identified as the decisive parameter causing the hourglass-shape of the spectrum.

PACS numbers: 75.20.-m, 71.10.-w, 75.47.Lx, 75.50.Ee, 75.25.+z

The implication of the stripe instability [1] in the pairing mechanism of high-temperature superconducting cuprates remains matter of strong controversy. Static stripe order competes with superconductivity in the cuprates, as superconductivity is strongly suppressed in samples with static stripe order [2]. However fluctuating stripes may coexist with good superconducting properties and could be important for the pairing. The shape of the dispersion of magnetic excitations in various superconducting cuprates [3–5] is taken as evidence that the stripe concept is the correct basis to understand the magnetic correlations even in highly doped cuprates, but analyzes within a fully itinerant picture also yield reasonable description [6]. At low energy, magnetic excitations can be associated with four incommensurate spots close to a common commensurate propagation vector, (0.5,0.5) [7]. With increasing energy the q-position varies little until a merging of different branches occurs at (0.5,0.5), which is associated with an enhanced signal. In constant energy maps at higher energy, the strongest scattering appears again at incommensurate positions, but intensity maxima are rotated by 45° with respect to those at low energy. This shape of the dispersion has been observed in several cuprates by now [3–5, 8].

Stripe phases were reported in other layered transition-metal oxides [9, 10]. Those appearing in isostructural nickelates [9] have been studied most, but the dispersion of magnetic excitations in these materials does not show the characteristic features of the hourglass dispersion [11] most likely due to the remarkable stability and particular ratio of interactions parameters of the magnetic order at 1/3 doping [11, 12]. More recently stripe-like magnetic ordering was also found in the layered isostructural cobaltates,  $\text{La}_{2-x}\text{Sr}_x\text{CoO}_4$  [10], and the magnetic excitations in one of these compounds,  $\text{La}_{1.67}\text{Sr}_{0.33}\text{CoO}_4$ , were found to exhibit a dispersion very similar to the hourglass dispersion in the cuprates [12].

Stripe phases have been reported also for manganites with a doping level above half doping [13–15]. In addition to the coupling of charges and magnetic moments in

cuprates and in nickelates, the orbital degrees of freedom are decisive in the manganites. Only recently a conclusive model of stripe-like magnetic and electronic ordering in manganites was elaborated by the aid of comprehensive neutron diffraction experiments [16]. In this work we analyze the magnetic excitations in two overdoped manganites with incommensurate magnetic order,  $\text{Nd}_{0.33}\text{Sr}_{1.67}\text{MnO}_4$  and  $\text{Pr}_{0.33}\text{Ca}_{1.67}\text{MnO}_4$ . Both compounds exhibit the characteristic features of the hourglass dispersion: the enhancement of signal at the merging of incommensurate branches, the rotation of the incommensurate intensity distribution with increasing energy and the suppression of the outwards dispersing signals. Most importantly, we find that the hourglass shape of the dispersion only appears for short magnetic correlation lengths.

Two large single-crystals of  $\text{Nd}_{0.33}\text{Sr}_{1.67}\text{MnO}_4$  and  $\text{Pr}_{0.33}\text{Ca}_{1.67}\text{MnO}_4$  have been grown by a floating-zone image furnace [17]. The quality of the samples has been checked by macroscopic and by microscopic investigations. Both systems exhibit a transition into a charge and orbital ordered state and, at lower temperatures, a transition into an antiferromagnetic state. The magnetic susceptibility of  $\text{Pr}_{0.33}\text{Ca}_{1.67}\text{MnO}_4$  measured in a SQUID magnetometer exhibits a clear kink at the transition into the charge and orbital ordered state at  $T=320\text{K}$  which is in perfect agreement with published data, [18] whereas the charge and orbital order in  $\text{Nd}_{0.33}\text{Sr}_{1.67}\text{MnO}_4$  is not visible in the susceptibility. The transitions into the antiferromagnetic state have been characterized by neutron diffraction on both compounds (Fig.1). Both systems exhibit nearly the same transition temperatures ( $T_N=100\text{K}$  for  $\text{Pr}_{0.33}\text{Ca}_{1.67}\text{MnO}_4$  and  $T_N=80\text{K}$  for  $\text{Nd}_{0.33}\text{Sr}_{1.67}\text{MnO}_4$ ), but the order is better defined in  $\text{Pr}_{0.33}\text{Ca}_{1.67}\text{MnO}_4$  which exhibits sharper magnetic superstructure peaks. The two compounds possess the same amount of electronic doping, but due to the smaller ionic radius of  $\text{Ca}^{2+}$   $\text{Pr}_{0.33}\text{Ca}_{1.67}\text{MnO}_4$  exhibits a structural distortion associated with the rotation of the  $\text{MnO}_6$  octahedra. Neutron-scattering experiments

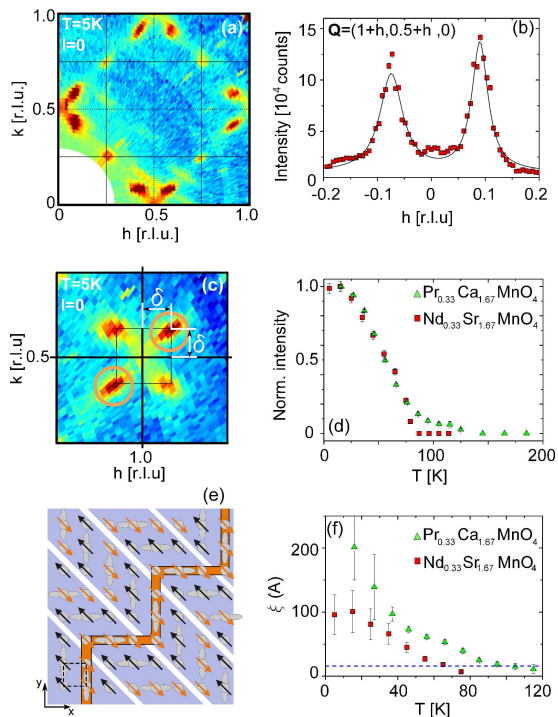


FIG. 1: (color online). Map of magnetic scattering in the  $(hk0)$ -plane in  $\text{Nd}_{0.33}\text{Sr}_{1.67}\text{MnO}_4$  at  $T=5\text{K}$  (a) and enlargement of the map (c) near  $\mathbf{Q}=(1.0,0.5)$ . Strong magnetic superstructure reflections are found near or at the positions of the magnetic intensities in half-doped  $\text{La}_{0.5}\text{Sr}_{1.5}\text{MnO}_4$ ; propagation vectors are  $\mathbf{k}_{Mn^{3+}} = \pm(0.25, 0.25, 0)$  and  $\mathbf{k}_{Mn^{4+}} = \pm(0.5 + \delta, \delta, 0)$  with  $\delta=0.083 \sim 1/12$ . (e) sketch of the orbital and magnetic structure explaining in 2/3-doped layered manganites; the slabs of strong magnetic correlations mediated through the orbital ordering are indicated by the diagonal ribbons. (b) Scan across two magnetic satellites and the common commensurate position. (d)  $(1,0.5)$  Peak height and (f) correlation length of the magnetic scattering along the modulation plotted as a function of temperature for the two compounds; the dashed line indicates the magnetic period which amounts to twice the distance of charge and orbital stripes.

were performed with the thermal spectrometers IN20 ( $k_f=3.00\text{\AA}^{-1}$ ) and IN3 ( $k_f=2.66\text{\AA}^{-1}$ ) at the ILL and 1T ( $k_f=2.66\text{\AA}^{-1}$ ) at the Orph ee reactor. In addition, the cold triple-axis instrument 4F.2 ( $k_f=1.55\text{\AA}^{-1}$ ) at LLB was used to study magnetic excitations at low energies.

Figure 1 shows a sketch of the magnetic order and a map of elastic scattering obtained in  $\text{Nd}_{0.33}\text{Sr}_{1.67}\text{MnO}_4$  at low temperature. For  $\text{Pr}_{0.33}\text{Ca}_{1.67}\text{MnO}_4$  we find very similar elastic patterns indicating essentially the same magnetic ordering. By comparison with the various types of order identified in slightly overdoped  $\text{La}_{0.42}\text{Sr}_{1.58}\text{MnO}_4$  [16] the different ordering patterns can be easily understood. The incommensurate superstructure intensities appearing at large  $\mathbf{Q}$ -vector can be identified with the orbital and charge order. In addition, there are two types of magnetic signals appearing at low  $\mathbf{Q}$ -values. The magnetic elastic scattering in  $\text{Pr}_{0.33}\text{Ca}_{1.67}\text{MnO}_4$  and in  $\text{Nd}_{0.33}\text{Sr}_{1.67}\text{MnO}_4$  differs from that in  $\text{La}_{0.42}\text{Sr}_{1.58}\text{MnO}_4$  as the incommen-

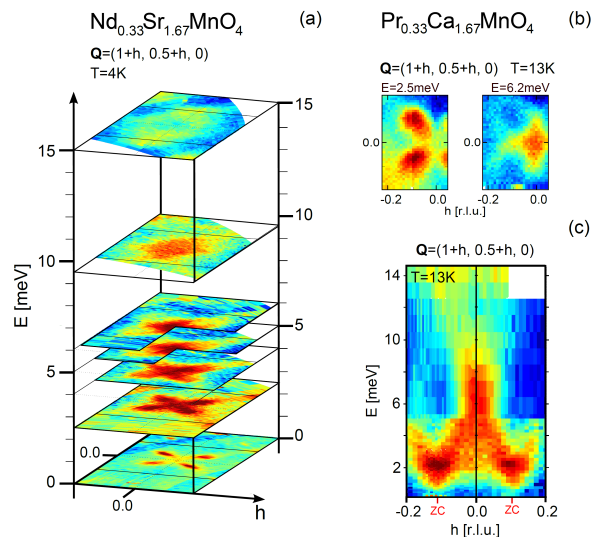


FIG. 2: (color online). Constant energy slices from  $\text{Nd}_{0.33}\text{Sr}_{1.67}\text{MnO}_4$  around the four incommensurate antiferromagnetic spots  $\mathbf{Q}=(1\pm\delta, 0.5\pm\delta, 0)$  with  $\delta=0.083$  measured at  $T=4\text{K}$  with the IN20 flatcone spectrometer (a). Two constant energy slices from  $\text{Pr}_{0.33}\text{Ca}_{1.67}\text{MnO}_4$  around the same incommensurate antiferromagnetic zone-centers  $\mathbf{Q}=(1\pm\delta, 0.5\pm\delta, 0)$  measured at  $T=13\text{K}$  with the 1T spectrometer (b). Part (c) shows an energy versus  $\mathbf{Q}$  map with the chosen  $\mathbf{Q}$ -direction passing across two incommensurate and the central commensurate positions. Data taken on the cold 4F.2 spectrometer and on the thermal 1T spectrometer were combined for this plot.

surate and commensurate scattering seems to be interchanged. In  $\text{Pr}_{0.33}\text{Ca}_{1.67}\text{MnO}_4$  and in  $\text{Nd}_{0.33}\text{Sr}_{1.67}\text{MnO}_4$  we find incommensurate signals close to the commensurate propagation vector of the order of  $\text{Mn}^{4+}$  moments in  $\text{La}_{0.5}\text{Sr}_{1.5}\text{MnO}_4$  [16, 19],  $\mathbf{Q}=(1\pm\delta, 0.5\pm\delta)$  with  $\delta=0.083$ . Four satellites are thus surrounding the commensurate center  $(1,0.5)$  similar to the arrangement of the incommensurate magnetic signal around  $\mathbf{Q}_{AFM}=(0.5,0.5)$  in the cuprates. In addition,  $\text{Pr}_{0.33}\text{Ca}_{1.67}\text{MnO}_4$  and  $\text{Nd}_{0.33}\text{Sr}_{1.67}\text{MnO}_4$  show commensurate signals exactly at the  $\mathbf{q}$ -position of the  $\text{Mn}^{3+}$  spin order in  $\text{La}_{0.5}\text{Sr}_{1.5}\text{MnO}_4$  [19]. Like in the case of  $\text{La}_{0.42}\text{Sr}_{1.58}\text{MnO}_4$ , the magnetic signals can be explained assuming that additional  $\text{Mn}^{4+}$  sites align in stripes along the diagonals, see the sketch in Fig. 1 (e). The magnetic order consists of an antiferromagnetic stacking of ferromagnetic zigzag chains similar to that in CE-type order at half doping. However, in contrast to the ideal CE-type order the legs of these ferromagnetic zigzag chains are four - and not three - units long.

Maps of inelastic scattering arising from the magnetic excitations are presented in Fig. 2 (a) and (b) for  $\text{Nd}_{0.33}\text{Sr}_{1.67}\text{MnO}_4$  and  $\text{Pr}_{0.33}\text{Ca}_{1.67}\text{MnO}_4$ , respectively. The  $(h,k)$  maps taken at constant energy transfer on  $\text{Nd}_{0.33}\text{Sr}_{1.67}\text{MnO}_4$  show that the elastic scattering and that at the low energy transfer of 2.5meV look qualitatively the same. At slightly higher energy, the incommensurate signals shift towards the commensurate po-

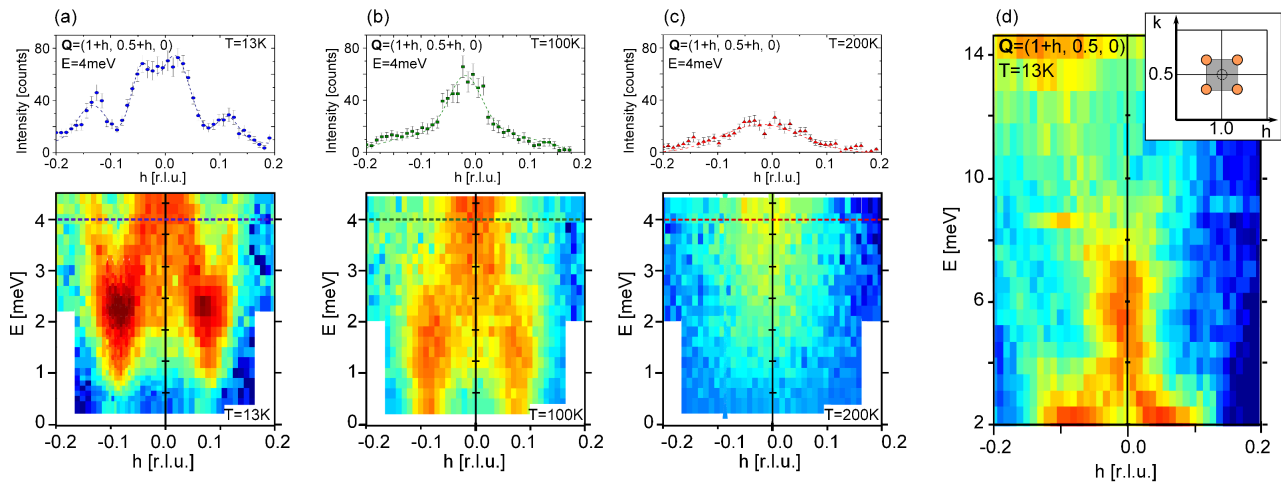


FIG. 3: (color online). [Lower panels (a-c)] energy-versus- $Q$  maps of the magnetic excitation spectrum in  $\text{Pr}_{0.33}\text{Ca}_{1.67}\text{MnO}_4$  at  $T=13$ K (a),  $T=100$ K (b) and  $T=200$ K (c) taken on the cold-source spectrometer 4F.2; the chosen  $Q$ -direction passes through the commensurate magnetic position  $(1.0, 0.5)$  and two incommensurate magnetic zone centers. [Upper panels (a-c)], constant energy cuts along the same  $Q$  path for an energy transfer of 4 meV; intensities were corrected for the Bose factor to simplify comparison. Map of magnetic excitations ( $Q$  versus energy) taken on the thermal spectrometer 1T (d); the chosen  $Q$ -direction passes through the commensurate magnetic position  $(0.5, 0.5)$  along  $Q=(1+h, 0.5, 0)$

sition where a single peak appears in the 6meV energy map. Further increase of the energy transfer results in a splitting of the signal. However, these intensity maxima appear now along the axes of the  $(h, k)$  plane and are thus rotated by  $45^\circ$  with respect to the low-energy ones. Fig. 2 (b) shows a map containing the energy and the  $Q$ -path cutting through two satellites and the commensurate center and energy cuts below and above the spin-wave merging. Fig. 3 shows the same maps at different temperatures and Fig. 4 an energy-versus- $Q$  map for the  $Q$ -path running through the commensurate center  $(0.5, 0.5)$  along the axis. Also this latter map shows the merging of spin-wave branches starting at the incommensurate satellites into the center.  $\text{Pr}_{0.33}\text{Ca}_{1.67}\text{MnO}_4$  exhibits qualitatively the same dispersion as  $\text{Nd}_{0.33}\text{Sr}_{1.67}\text{MnO}_4$ , but we already want to emphasize that the  $\text{Pr}_{0.33}\text{Ca}_{1.67}\text{MnO}_4$  map taken at low temperature also exhibits outwards dispersing branches. Only at higher temperature, when the correlation length has become shorter, these outwards branches are suppressed giving rise to the full hourglass shape. The shape of the dispersion in both these insulating materials strongly resembles the hourglass distribution in the cuprates [4, 5] as it was also reported for  $\text{La}_{2-x}\text{Sr}_x\text{CoO}_4$  [12]. This is most visible in the enhancement of the signal towards the commensurate center and in the rotation of the position of the satellites with increasing energy. The hourglass dispersion can thus be considered as the normal result of a stripe arrangement with short correlation length, and the nickelates case appears special most likely due to the particular stability of this magnetic phase [11]. In the manganites the scattering at the incommensurate satellites exhibits a clear gap due to single-ion anisotropy similar to behavior in the half-doped compounds [19, 20] rendering this dispersion even more similar to that in the cuprates.

The similarities between the hourglass shape of mag-

netic excitations in metallic cuprates and the dispersion arising from an incommensurate insulating stripe phase is remarkable, but it does not fully exclude other explanations of the magnetic response in the cuprates [6]. In particular the resonance mode in the superconducting phase in cuprates requires further attention.

We have also studied the magnetic excitations in  $\text{La}_{0.42}\text{Sr}_{1.58}\text{MnO}_4$  finding again an hourglass type of dispersion at low energies. Due to the much smaller pitch of the incommensurate modulation in  $\text{La}_{0.42}\text{Sr}_{1.58}\text{MnO}_4$  the merging of the spin-wave branches appears at much lower energy, so that a high energy resolution is required strongly limiting the statistics.

Some of the features of the hourglass dispersion can be well described within linear spin-wave theory [21]. For example the merging of the branches and the rotation of the incommensurate scattering in constant energy cuts above the merging are just consequences of the dispersion of the branches starting at different satellites. However spin-wave theory predicts that both the inwards and the outwards dispersing branches starting from the satellites possess considerable intensity. In contrast, the hourglass spectrum gains its characteristic shape by the suppression of the outwards dispersing branches. In the magnetic response of the cuprates there is no indication of these branches left. In this aspect the low-temperature spectrum in  $\text{Pr}_{0.33}\text{Ca}_{1.67}\text{MnO}_4$  looks different, as one can clearly identify the outwards dispersing branches as well. These outwards modes present a significant difference to the hourglass spectrum in the cuprates. By varying the temperature,  $\text{Pr}_{0.33}\text{Ca}_{1.67}\text{MnO}_4$  offers the possibility to analyze the origin of this important aspect of the hourglass spectrum. At the intermediate temperature of 100 K the outwards modes are severely suppressed, so that the magnetic response of  $\text{Pr}_{0.33}\text{Ca}_{1.67}\text{MnO}_4$  becomes fully similar to the hourglass spectrum. Further

increase of the temperature up to 200 K reduces the signs of the incommensurate scattering in this inelastic energy-versus- $Q$  map. In  $\text{Pr}_{0.33}\text{Ca}_{1.67}\text{MnO}_4$ , the suppression of the outwards branches clearly follows the reduction of the correlation length perpendicular to the stripes shown in Fig. 1(f). In  $\text{Nd}_{0.33}\text{Sr}_{1.67}\text{MnO}_4$  the correlation length of magnetic ordering across the stripes remains reduced even at the lowest temperature in accordance with a pronounced hourglass shape persisting. We may thus conclude that the correlation length of the magnetic stripe order has an essential impact on the shape of the magnetic response. For long correlation lengths, as present at low temperature in  $\text{Pr}_{0.33}\text{Ca}_{1.67}\text{MnO}_4$ , the outwards and the inwards dispersing branches possess comparable weight, whereas the response focusses into the inwards dispersing branches for shorter correlation lengths.

When the hourglass-shaped dispersion is observed, both manganites exhibit very short longitudinal magnetic correlation lengths, of the order of or even below the length of the magnetic period (i.e. twice the stripes distance), whereas the correlation of the orbital order is still sizeable. A smoothly decaying magnetic order parameter is no longer appropriate to describe such short range magnetic ordering, but one may conclude that magnetically correlated regions cover only a few charge stripes in these states in spite of a well defined modulation direction. This is reminiscent of a nematic state [22].

The reason for the short correlation length in the two 2/3-doped manganites can be understood by inspecting Fig. 1(e). Orbital ordering forms slabs running along the diagonals. In these three-Mn thick slabs the magnetic order is well determined: the orientation of the ordered  $e_g$  orbital couples the moments of the two  $\text{Mn}^{4+}$  ferromagnetically with the central  $\text{Mn}^{3+}$  moment; neighboring  $\text{Mn}^{4+}$ - $\text{Mn}^{3+}$ - $\text{Mn}^{4+}$  trimers are coupled antiferromagnetically, so that all moments within a slab are well fixed by magnetic interaction parameters that can be expected being very similar to those in  $\text{La}_{0.5}\text{Sr}_{1.5}\text{MnO}_4$  [23]. The slabs are indicated as shaded areas in Fig. 1 (e). However, the interaction between two slabs is frustrated in the ideal tetragonal structure, and some additional distortion is needed to stabilize the four-leg zigzag structure. The weak inter-slab interaction causes the rapid melting of magnetic order much below the suppression of orbital ordering. It is the state with loosely coupled magnetic slabs, which exhibits the hourglass dispersion. This situation is very similar to the short-range magnetic order in  $\text{La}_{1.67}\text{Sr}_{0.33}\text{CoO}_4$  [10, 12] and in cuprates. In both these cases magnetic coupling across the stripes is very weak compared to the nearest-neighbor coupling active within the antiferromagnetic regions. The hourglass spectrum in the cuprates was analyzed in various models for itinerant or local moments with or without static order [24–26]. The model of weakly coupled ladders corresponds to a very short correlation length of only one ladder size and results in the suppression of the outwards modes [24]. In contrast, the strong coupling across the charge stripe in the nickelates results in more stable magnetic order [11] reflected by an isotropic spin-wave dispersion.

In conclusion the dispersion of magnetic excitations in strongly overdoped layered manganites closely resembles the hourglass spectrum seen in the cuprates and in a layered cobaltate. Some of the characteristic hourglass features can be attributed to the incommensurate modulation of the magnetism in these stripe phases. These are the enhanced signal at the merging point of the branches and the rotation of the incommensurate signal in constant energy maps. However, the suppression of the outwards-dispersing branches, which is the essential element of the hourglass spectrum, can be attributed to the reduction of the correlation lengths. In  $\text{Pr}_{0.33}\text{Ca}_{1.67}\text{MnO}_4$ , we find significant intensity in the outwards dispersing branches at low temperature, where the correlation lengths are long. These branches, however, become suppressed upon heating and decrease of the correlation lengths, giving rise to the hourglass spectrum. In the cuprates, in the cobaltate and in the manganites studied here, the hourglass dispersion thus appears in a state with slabs of well defined magnetic correlations, which are only loosely coupled.

This work was supported by the Deutsche Forschungsgemeinschaft through the Sonderforschungsbereich 608.

---

\* Electronic address: ulbrich@ph2.uni-koeln.de

† Electronic address: braden@ph2.uni-koeln.de

- [1] J.M. Tranquada *et al.*, Nature (London) **375**, 561 (1995).
- [2] N. Ichikawa *et al.*, Phys. Rev. Lett. **85**, 1738 (2000); J. M. Tranquada *et al.*, Phys. Rev. Lett. **78**, 338 (1997).
- [3] M. Arai *et al.*, Phys. Rev. Lett. **83**, 608 (1999).
- [4] J.M. Tranquada, *et al.*, Nature **429**, 534 (2004).
- [5] S. Hayden *et al.*, Nature **429**, 531 (2004).
- [6] M. Eschrig, Adv. Phys. **55**, 47 (2006).
- [7] Throughout this paper, we use two-dimensional notations neglecting the weak inter-layer coupling ( $a \sim 3.8\text{\AA}$ ).
- [8] Hinkov *et al.*, Nat. Phys. **3**, 780 (2007); O. J. Lipscombe *et al.*, Phys. Rev. Lett. **99**, 067002 (2007); Guangyong Xu *et al.*, Phys. Rev. B **76**, 014508 (2007).
- [9] J.M. Tranquada *et al.*, Phys. Rev. B **54**, 12318 (1996).
- [10] M. Cwik *et al.*, Phys. Rev. Lett. **102**, 057201 (2009).
- [11] P. Bourges *et al.*, Phys. Rev. B. **90**, 147202 (2003).
- [12] A.T. Boothroyd *et al.*, Nature **471** 341 (2011).
- [13] A.P. Ramirez *et al.*, Phys. Rev. Lett. **76**, 3188 (1996).
- [14] C.H. Chen *et al.*, J. Appl. Phys. **81**, 4326 (1997).
- [15] S. Mori *et al.*, Nature **392**, 473 (1998).
- [16] H. Ulbrich *et al.*, Phys. Rev. Lett. **106**, 157201 (2011).
- [17] P. Reutler *et al.*, J. Cryst. Growth **249**, 222 (2003).
- [18] R. Mathieu and Y. Tokura, J. Phys. Soc., **76**, 12 (2007).
- [19] D. Senff *et al.*, Phys. Rev. B. **77**, 184413 (2008).
- [20] H. Ulbrich *et al.*, Phys. Rev. B **84**, 094453 (2011).
- [21] F. Krüger and S. Scheidl, Phys. Rev. B **67**, 134512 (2003); E.W. Carlson *et al.*, Phys. Rev. B **70**, 064505 (2004).
- [22] S.A. Kivelson *et al.*, Rev. Mod. Phys. **75**, 1201 (2003).
- [23] D. Senff *et al.*, Phys. Rev. Lett. **96**, 257201 (2006).
- [24] G.S. Uhrig *et al.*, Phys. Rev. Lett. **93**, 267003 (2004).
- [25] G. Seibold and J. Lorenzana, Phys. Rev. Lett. **94**, 107006 (2005).
- [26] M. Vojta *et al.*, Phys. Rev. Lett. **99**, 097001 (2006).